

Nanoscale

Accepted Manuscript



This is an *Accepted Manuscript*, which has been through the Royal Society of Chemistry peer review process and has been accepted for publication.

Accepted Manuscripts are published online shortly after acceptance, before technical editing, formatting and proof reading. Using this free service, authors can make their results available to the community, in citable form, before we publish the edited article. We will replace this *Accepted Manuscript* with the edited and formatted *Advance Article* as soon as it is available.

You can find more information about *Accepted Manuscripts* in the [Information for Authors](#).

Please note that technical editing may introduce minor changes to the text and/or graphics, which may alter content. The journal's standard [Terms & Conditions](#) and the [Ethical guidelines](#) still apply. In no event shall the Royal Society of Chemistry be held responsible for any errors or omissions in this *Accepted Manuscript* or any consequences arising from the use of any information it contains.

Cite this: DOI: 10.1039/c0xx00000x

www.rsc.org/xxxxxx

ARTICLE TYPE

Reversible Formation of Ag₄₄ from Selenolates†

Indranath Chakraborty and T. Pradeep*

Received (in XXX, XXX) Xth XXXXXXXXXX 20XX, Accepted Xth XXXXXXXXXX 20XX

DOI: 10.1039/b000000x

The cluster Ag₄₄SePh₃₀, originally prepared from silver selenolate, upon oxidative decomposition by H₂O₂ makes the same cluster back, in an apparently reversible synthesis. Such an unusual phenomenon was not seen for the corresponding thiolate analogues. From several characterization studies such as mass spectrometry, Raman spectroscopy, etc., it has been confirmed that the degraded and as-synthesized selenolates are the same in nature, which leads to the reversible process. Possibility of making clusters from the degraded material makes cluster synthesis economical. This observation makes one consider cluster synthesis to be a reversible chemical process, at least for selenolates.

Synthesis and characterisation of noble metal quantum clusters is becoming one of the most fascinating topics of materials research due to their unique size-dependent properties.¹⁻⁵ Ultra small size and enhanced optical properties make them widely applicable in a variety of applications such as surface enhanced Raman scattering (SERS),⁶ catalysis,⁷ bio-labelling,^{8, 9} sensing^{10, 11} and many others.¹²⁻¹⁴

Starting from the Brust protocol,¹⁵ several synthetic routes such as modified Brust synthesis,^{16, 17} high temperature route,¹⁸ solid state route,¹⁹⁻²² interfacial synthesis,²³ etc. have been developed to create such atomically precise pieces of matter. As of now, most of the reports are on gold clusters and crystal structures of Au₂₃,²⁴ Au₂₄,²⁵ Au₂₅,^{5, 26} Au₂₈,²⁷ Au₃₀,²⁸ Au₃₆,²⁹ Au₃₈,^{30, 31} and Au₁₀₂³² have been reported. Compared to gold, very few reports exist for silver clusters^{33, 34} with detailed characterization, which include Ag_{7,8},²³ Ag₉,²⁰ Ag₃₂,³⁵ Ag₄₄³⁶ and Ag₁₅₂.¹⁹ Crystal structures of mixed ligand protected Ag₁₄,³⁷ Ag₁₆³⁸ and Ag₃₂³⁸ clusters have been solved. Recently, crystal structure of the very first complete thiolate protected Ag₄₄ clusters has been reported from Bigioni³⁹ and Zheng⁴⁰ groups. The Ag₄₄(SR)₃₀ cluster forms a Keplerate solid of concentric icosahedral and dodecahedral atom shells to form a hollow cage which is further protected by six Ag₂(SR)₅ units in an octahedral geometry. A similar structure has been proposed for the selenolate analogue of the Ag₄₄ cluster⁴¹ which shows an identical optical spectrum with a shift, as expected from the difference in ligand. In most of the cases, the clusters have been examined in terms of their stability.⁴²⁻⁴⁴ As silver clusters are easily oxidisable under aerobic conditions, they degrade rapidly to form thiolates or selenolates and studies on

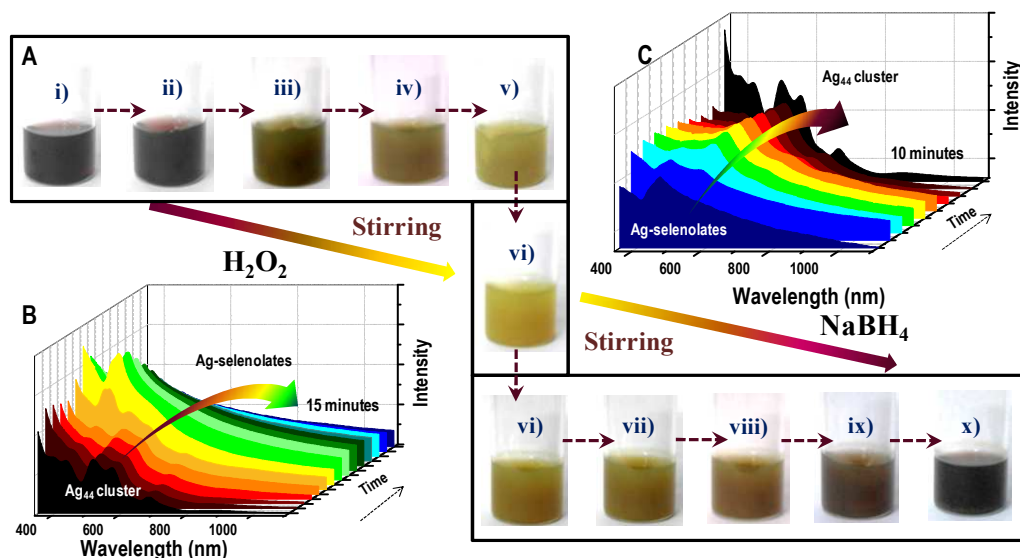


Fig. 1. A: Photographs of the Ag₄₄(SePh)₃₀ cluster solution showing time dependent changes during oxidation (i to vi) and reduction (vi to x). Oxidation was accomplished by H₂O₂ and reduction was by NaBH₄. B: Time dependent UV/Vis spectra during oxidation of Ag₄₄ cluster to form selenolates. C: Time dependent UV/Vis spectra for the reduction of selenolates to form the Ag₄₄ cluster. Each spectrum has been collected at 1 min interval.

intact clusters are limited.

In this work, we report the reversible formation of Ag_{44} cluster from selenolates. The reversibility has been checked for corresponding other clusters also but interestingly, except selenolated Ag_{44} , no other systems (including thiolated Ag_{44} , which is chemically most similar) show this property. The clusters examined include, $\text{Ag}_{44}(\text{SPh})_{30}$, $\text{Ag}_{44}(4\text{-FTP})_{30}$, and $\text{Ag}_{44}(3\text{-FTP})_{30}$ where SPh, 4-FTP and 3-FTP corresponds to the thiolate forms of thiophenol, 4-fluorothiophenol and 3-fluorothiophenol, respectively. A larger silver cluster, $\text{Ag}_{152}(\text{PET})_{60}$ was also studied. To explore this phenomenon in more detail, we have oxidised the cluster using peroxide to form selenolates and then the reversibility was checked using borohydride reduction. Several other characterisation studies were done to understand the reversibility.

A two phase solution state route as described in our previous report⁴¹ has been used to synthesize the cluster. Initially, silver trifluoroacetate (0.0714 mmol) was dissolved in 7.2 mL acetonitrile and stirred for 5 min. Benzeneselenol (0.0471 mmol) was added to that solution and was left to stir for another 15 min (resulting in solution A). In another conical flask, 28.6 mL acetonitrile solution of NaBH_4 (0.286 mmol) was kept for stirring for 30 min (solution B). Then, solution B was added to solution A and the reaction mixture was left to stir for 3 h at room temperature. Purple colored cluster was formed after 3 h and it was stored in a refrigerator at $\sim 4^\circ\text{C}$. Similar methodologies have been followed for thiol protected clusters also. More details are given in the supporting information.

The $\text{Ag}_{44}(\text{SePh})_{30}$ cluster⁴¹ shows five intense bands at 1.41 (879), 1.82 (681), 2.16 (574), 2.40 (516) and 2.82 (440) eV (nm) along with three broad bands centered around 1.27 (970), 1.95 (635) and 3.14 (395) eV (nm) in its absorption spectrum. The cluster kept in aerobic condition will lose its optical identity gradually and a yellow precipitate appears. Reversible cluster formation was observed first from the degraded cluster. Upon addition of adequate amount of borohydride and constant stirring, we observed that the degraded selenolate, formed from the cluster (*selenolate I*) can be reformed to the Ag_{44} cluster in 10 minutes. However, degradation under aerobic condition typically takes 5-7 days and time dependent observation was difficult. So, an external oxidizing agent, hydrogen peroxide, was added to a controlled amount so that we can monitor oxidation in real time. Photographs at different stages of the reaction are given in Fig. 1A. The cluster is deep pink in color but upon addition of H_2O_2 , the color changes to yellowish-brown and finally to yellow which confirms the formation of silver selenolate. The reaction was monitored through absorption spectroscopy where the distinct features of $\text{Ag}_{44}(\text{SePh})_{30}$ cluster are lost and subsequently a new peak around 450 nm along with a hump at 430 nm started appearing, due to selenolate. As time progresses, the baseline of the spectrum started increasing because of the low solubility of selenolate in acetonitrile. During the reduction of this *selenolate I* with NaBH_4 , the color changes in reverse order and finally the solution becomes clear and attains wine red color which confirms the formation of Ag_{44} cluster. The corresponding UV/Vis spectra are given in Fig. 1C where the spectra also change in reverse order. The sharp selenolate peak disappears and all the features of Ag_{44} started appearing with time. The reaction time is controlled by the concentration of the cluster, the amount of H_2O_2 and NaBH_4 . Constant stirring is also important for this case. For more clarity, these reversible cycles are shown by selecting the intensity of the 516 nm peak for five consecutive cycles (Fig. S1, ESI[†]).

Similar experiments have been tried for $\text{Ag}_{44}(\text{SPh})_{30}$ which is the thiol analogue of $\text{Ag}_{44}(\text{SePh})_{30}$. For this cluster, upon addition of H_2O_2 (all concentrations were kept

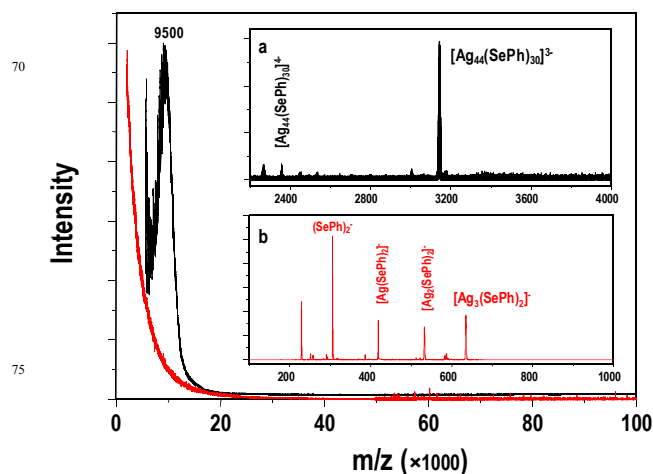


Fig. 2. MALDI MS data of $\text{Ag}_{44}(\text{SePh})_{30}$ cluster (black trace) and *selenolate I* (red trace). Inset shows the ESI mass spectra of Ag_{44} cluster (a) and *selenolate I* (b), respectively. All the peaks are marked.

constant) thiolates were formed, as expected. The UV/Vis spectra (Fig. S2A, ESI[†]) clearly show a sharp peak near 350 nm corresponding to thiolates and the features of $\text{Ag}_{44}(\text{SPh})_{30}$ cluster have been lost completely. Reduction of this degraded thiolate (*thiolate I*) has resulted in a broad hump near 400 nm and the cluster feature was not developed suggesting that the system was not reversible. We have studied $\text{Ag}_{44}(4\text{-FTP})_{30}$ (Fig. S2B, ESI[†]) and $\text{Ag}_{44}(3\text{-FTP})_{30}$ (Fig. S2C, ESI[†]) also but they both do not show the reversible formation. The ' $\text{Ag}_{44}(4\text{-FTP})_{30}$ derived thiolate' form nanoparticles by reduction. The plasmonic feature can be seen in the optical spectrum (Fig. S2B, ESI[†]) while a hump at 480 nm can be observed in the case of ' $\text{Ag}_{44}(3\text{-FTP})_{30}$ -derived thiolate' under the same condition. Degradation to thiolate is not reversible in the larger cluster, $\text{Ag}_{152}(\text{PET})_{60}$ (Fig. S3, ESI[†]). In the cluster literature, the only case of reversibility observed was by Anand *et al.*⁴⁵ who reported the reversible transformation of human serum albumin protected Ag_9 to Ag_{14} cluster. Note that the cluster core changes during this transformation. Therefore, the reversibility seen in the case of $\text{Ag}_{44}(\text{SePh})_{30}$ is unprecedented. As Au clusters are different chemically in most of their properties,⁴⁶ a similar study was not attempted on them.

To find the reason for this unique transformation, detailed characterization of *selenolate I* was performed. Initially, matrix assisted laser desorption ionization mass spectrometry (MALDI MS) was performed for the cluster as well as *selenolate I* (Fig. 2). $\text{Ag}_{44}(\text{SePh})_{30}$ shows a peak centered around m/z 9500 using DCTB as the matrix^{19, 33, 34} and as expected, *selenolate I* does not show any feature. Electrospray ionization mass spectrometry (ESI MS) shows 3-, 4- features (Fig. 2a) of $\text{Ag}_{44}(\text{SePh})_{30}$ which confirm the purity of the cluster. As selenolates have very less solubility, methanol-acetonitrile mixture was used for the ESI measurement. Some selenolate species such as $\text{Ag}_3(\text{SePh})_2$, $\text{Ag}_2(\text{SePh})_2$ and $\text{Ag}(\text{SePh})_2$ have been observed in the negative ion mode. For confirmation, ESI MS was also taken for the reversibly formed Ag_{44} cluster which shows the same feature as depicted in Fig. 2A.

We thought that comparison of *selenolate 1* with the as-synthesized selenolate (*selenolate 2*) and similar thiolate samples (synthesis procedures are given in supporting information) might be useful to understand this phenomenon. UV/Vis spectroscopy for both the cases have been compared (Fig. S4, ESI†) and it was found that for the case of selenolate, the spectra are comparable (Fig. S4A, ESI†) but drastic differences are there for thiolates (Fig. S4B, ESI†). As-synthesized thiolate (*thiolate 2*) shows a sharp peak at 237 nm and a broad hump at 277 nm whereas *thiolate 1* shows four broad humps at 240, 280, 360 and 420 nm, respectively. *Selenolate 1* shows a peak at 464 nm along with a hump at 430 nm and similar two peaks at 430 and 450 nm were observed for *selenolate 2*. So, *selenolate 1* and *2* might be the same as it appears in absorption spectroscopy. To understand it better, laser desorption ionization mass spectrometric (LDI MS) analysis was attempted for the thiolates

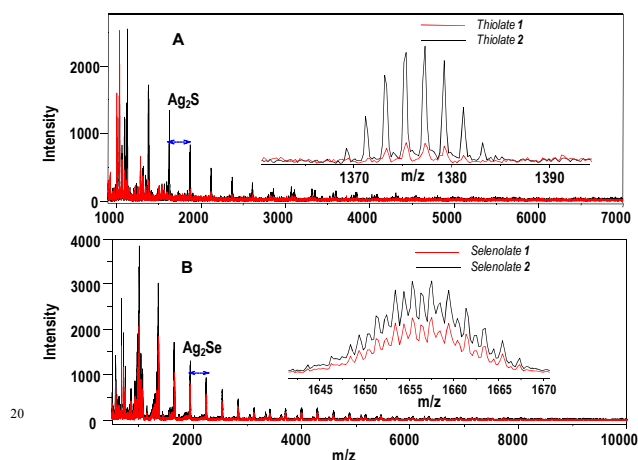


Fig. 3. Comparative LDI mass spectra of thiolates (A) and selenolates (B). Insets for both the cases show an extended view of some selected peaks centred at m/z 1377 (for thiolates) and m/z 1656 (for selenolates). True ion intensities are compared and not relative abundances.

and selenolates (Fig. 3). It is important to mention here that LDI MS has been used as these thiolates and selenolates have very less solubility, so it was difficult to do electrospray ionization (ESI) or matrix assisted laser desorption ionization (MALDI) mass analysis. Here also similar trends have been observed as seen in absorption spectroscopy. Systematic Ag_2S losses have been observed for both the thiolates (Fig. 3A) but the loss started from higher mass (m/z 4500) for *thiolate 2* while it started from m/z 1800 for *thiolate 1*, that too with much lower intensity (an expanded view of a peak at m/z 1375 is shown in the inset of Fig. 3A). Interestingly, in the lower mass, intensity gradually increases for *thiolate 2* and some shift has also been observed. The data suggest that *thiolate 1* and *2* are different in nature. Selenolates show similar feature and systematic Ag_2Se losses have been seen (Fig. 3B) from almost the same mass region and the isotope pattern is also the same (inset of Fig 3B). The reason for the complicated fine structure of selenolates compared to thiolates is because of the isotopes of Se. Selenium has six isotopes namely, ^{74}Se (0.89 %), ^{76}Se (9.37 %), ^{77}Se (7.63 %), ^{78}Se (23.77 %), ^{80}Se (49.61 %), and ^{82}Se (8.73 %) which contribute significantly to the fine mass spectral features compared to sulfur which has only one predominant isotope, namely ^{32}S (95 %). Raman spectroscopy was used to confirm that selenolates are the same but thiolates are different in nature (Fig. S5, ESI†). Although detailed peak assignments have not been done, many

are assigned based on the literature.⁴⁷ From a comparative study, we can see that Raman features for *selenolate 1* and *2* (Fig. S5A, ESI†) are the same but differences are there for thiolates (Fig. S5, ESI†). The peak at 1070 cm^{-1} (ring deformation mode⁴⁷) for *thiolate 1* has been split for *thiolate 2* along with some more additional peaks near 1020 cm^{-1} (ring breathing mode⁴⁷). Differences were observed for thiolates in SEM images (Fig. S6, ESI†). As-synthesized thiolates appear amorphous whereas degraded one shows crystalline nature. For the case of selenolates, both of them show porous structure (Fig. S6, ESI†). From the SEM/EDAX analysis, the ratio of Ag:Se for the degraded selenolate species is found as 1:0.68 (3:2.04) which is very close to the atomic ratios present in the cluster (Fig. S7, ESI†). Non-stoichiometry in thiolates was found earlier⁴⁸⁻⁵¹ and similar case is expected for selenolates also. Parikh *et al.* have shown the existence of silver rich thiolates using elemental analysis.⁵² Li *et al.*^{48, 49} and Sun *et al.*⁵⁰ have shown the crystal structures of metal rich thiolates. McLauchlan and Ibers have shown sulphur and selenium rich silver thiolates.⁵³ So it is not difficult to rationalize the existence of non-stoichiometric thiolates or selenolates in our experiments. In detail such thiolates may be structures with sulphide cores with thiolate shell, although the authors refer to them as thiolates.

From all these data it is confirmed that degraded and as-synthesized selenolates are the same in nature and because of that formation of $\text{Ag}_{44}\text{SePh}_{30}$ is reversible. Another reason for the reversibility could be the higher stability of this selenolate protected Ag_{44} cluster compared to the thiol protected one. To confirm this, the cluster has been synthesized with different concentrations of benzeneselenol and surprisingly, all of them resulted in Ag_{44} cluster with distinct optical and mass spectral features (Fig. S8, ESI†). The cluster has been synthesized at different temperatures and surprisingly, in all the cases (from 0-60 °C) they were formed (Fig. S9, ESI†) which suggests the high stability of the system. Formation time of the cluster reduced drastically with increase in temperature, which is expected (inset of Fig. S9, ESI†). For the thiol case, irreversibility has been observed because of the different nature of the thiolates and may be upon reduction, thiolates have many possibilities to make diverse clusters or bigger nanoparticles.

In summary, we have synthesized selenolate and thiolate analogues of Ag_{44} clusters using similar synthetic methodologies. Unusual reversible formation of Ag_{44} cluster from selenolate was observed. This phenomenon has not been seen for the corresponding thiolates. Several characterization techniques have been used to understand the reversibility. It has been found that degraded selenolates and as-synthesized selenolates are the same in nature but they are different in the case of thiolates which is responsible for this unusual property. This opens up a new possibility of making clusters from the degraded materials which may be economical for precious metals like gold and silver. Most important aspect of this finding appears to be that cluster synthesis is proven to be reversible, at least in the limited case of selenolates. This suggests that clusters may be treated just as molecules in their chemistry.

We thank the Department of Science and Technology, Government of India for constantly supporting our research program on nanomaterials. I.C. thanks IITM for research fellowships.

Notes and references

*DST Unit of Nanoscience (DST UNS) and Thematic Unit of Excellence (TUE), Department of Chemistry, Indian Institute of

Technology Madras, Chennai 600 036, India; Fax: 91-44-2257 0545; E-mail: pradeep@iitm.ac.in

† Electronic Supplementary Information (ESI) available: [Details of experimental procedures; instrumentation; reversible cycles, UV/Vis spectra of thiophenol, 4-FTP, 3-FTP protected Ag₄₄, and Ag₁₅₂ cluster; UV/Vis, SEM images and Raman spectra of as-synthesized and degraded thiolates & selenolates; SEM/EDAX of degraded selenolates, UV/Vis of Ag₄₄(SePh)₃₀ cluster under different selenol concentrations and temperatures] See DOI: 10.1039/b000000x/.

1. C. M. Aikens, *J. Phys. Chem. C*, 2008, **112**, 19797-19800.
2. T. P. Bigioni, R. L. Whetten and Ö. Dag, *J. Phys. Chem. B*, 2000, **104**, 6983-6986.
3. S. Link, A. Beeby, S. FitzGerald, M. A. El-Sayed, T. G. Schaaff and R. L. Whetten, *J. Phys. Chem. B*, 2002, **106**, 3410-3415.
4. K. Nobusada and T. Iwasa, *J. Phys. Chem. C*, 2007, **111**, 14279-14282.
5. M. Zhu, C. M. Aikens, F. J. Hollander, G. C. Schatz and R. Jin, *J. Am. Chem. Soc.*, 2008, **130**, 5883-5885.
6. I. Chakraborty, S. Bag, U. Landman and T. Pradeep, *J. Phys. Chem. Lett.*, 2013, **4**, 2769-2773.
7. S. Yamazoe, K. Koyasu and T. Tsukuda, *Acc. Chem. Res.*, 2014, **47**, 816-824.
8. C.-A. J. Lin, T.-Y. Yang, C.-H. Lee, S. H. Huang, R. A. Sperling, M. Zanella, J. K. Li, J.-L. Shen, H.-H. Wang, H.-I. Yeh, W. J. Parak and W. H. Chang, *ACS Nano*, 2009, **3**, 395-401.
9. M. A. H. Muhammed and T. Pradeep, in *Advanced Fluorescence Reporters in Chemistry and Biology II*, ed. A. P. Demchenko, Springer Berlin Heidelberg, 2010, vol. 9, ch. 11, pp. 333-353.
10. I. Chakraborty, T. Udayabhaskararao and T. Pradeep, *J. Hazard. Mater.*, 2012, **211-212**, 396-403.
11. A. Mathew, P. R. Sajanalal and T. Pradeep, *Angew. Chem. Int. Ed.*, 2012, **51**, 9596-9600.
12. I. Chakraborty, T. Udayabhaskararao, G. K. Deepesh and T. Pradeep, *J. Mater. Chem. B*, 2013, **1**, 4059-4064.
13. T. Chen, S. Xu, T. Zhao, L. Zhu, D. Wei, Y. Li, H. Zhang and C. Zhao, *ACS Appl. Mater. Inter.*, 2012, **4**, 5766-5774.
14. Y. Kong, J. Chen, F. Gao, R. Brydson, B. Johnson, G. Heath, Y. Zhang, L. Wu and D. Zhou, *Nanoscale*, 2013, **5**, 1009-1017.
15. M. Brust, M. Walker, D. Bethell, D. J. Schiffrin and R. Whyman, *J. Chem. Soc., Chem. Commun.*, 1994, 801-802.
16. S. Gaur, J. T. Miller, D. Stellwagen, A. Sanampudi, C. S. S. R. Kumar and J. J. Spivey, *Phys. Chem. Chem. Phys.*, 2012, **14**, 1627-1634.
17. J. Kim, K. Lema, M. Ukaigwe and D. Lee, *Langmuir*, 2007, **23**, 7853-7858.
18. I. Chakraborty, T. Udayabhaskararao and T. Pradeep, *Chem. Commun.*, 2012, **48**, 6788-6790.
19. I. Chakraborty, A. Govindarajan, J. Erusappan, A. Ghosh, T. Pradeep, B. Yoon, R. L. Whetten and U. Landman, *Nano Lett.*, 2012, **12**, 5861-5866.
20. T. U. B. Rao, B. Nataraju and T. Pradeep, *J. Am. Chem. Soc.*, 2010, **132**, 16304-16307.
21. I. Chakraborty, R. G. Bhuin, S. Bhat and T. Pradeep, *Nanoscale*, 2014, **6**, 8561-8564.
22. A. Ganguly, I. Chakraborty, T. Udayabhaskararao and T. Pradeep, *J. Nanopart. Res.*, 2013, **15**, 1-7.
23. T. Udaya Bhaskara Rao and T. Pradeep, *Angew. Chem. Int. Ed.*, 2010, **49**, 3925-3929.
24. A. Das, T. Li, K. Nobusada, C. Zeng, N. L. Rosi and R. Jin, *J. Am. Chem. Soc.*, 2013, **135**, 18264-18267.
25. A. Das, T. Li, K. Nobusada, Q. Zeng, N. L. Rosi and R. Jin, *J. Am. Chem. Soc.*, 2012, **134**, 20286-20289.
26. M. W. Heaven, A. Dass, P. S. White, K. M. Holt and R. W. Murray, *J. Am. Chem. Soc.*, 2008, **130**, 3754-3755.
27. C. Zeng, T. Li, A. Das, N. L. Rosi and R. Jin, *J. Am. Chem. Soc.*, 2013, **135**, 10011-10013.
28. D. Crasto, S. Malola, G. Brosofsky, A. Dass and H. Häkkinen, *J. Am. Chem. Soc.*, 2014, **136**, 5000-5005.
29. C. Zeng, H. Qian, T. Li, G. Li, N. L. Rosi, B. Yoon, R. N. Barnett, R. L. Whetten, U. Landman and R. Jin, *Angew. Chem. Int. Ed.*, 2012, **51**, 13114-13118.
30. Y. Pei, Y. Gao and X. C. Zeng, *J. Am. Chem. Soc.*, 2008, **130**, 7830-7832.
31. H. Qian, W. T. Eckenhoff, Y. Zhu, T. Pintauer and R. Jin, *J. Am. Chem. Soc.*, 2010, **132**, 8280-8281.
32. P. D. Jadzinsky, G. Calero, C. J. Ackerson, D. A. Bushnell and R. D. Kornberg, *Science*, 2007, **318**, 430-433.
33. I. Chakraborty, J. Erusappan, A. Govindarajan, K. Sugi, T. Udayabhaskararao, A. Ghosh and T. Pradeep, *Nanoscale*, 2014, **6**, 8024-8031.
34. K. S. Sugi, I. Chakraborty, T. Udayabhaskararao, J. S. Mohanty and T. Pradeep, *Part. Part. Sys. Charac.*, 2013, **30**, 241-243.
35. J. Guo, S. Kumar, M. Bolan, A. Desireddy, T. P. Bigioni and W. P. Griffith, *Anal. Chem.*, 2012, **84**, 5304-5308.
36. K. M. Harkness, Y. Tang, A. Dass, J. Pan, N. Kothalawala, V. J. Reddy, D. E. Cliffler, B. Demeler, F. Stellacci, O. M. Bakr and J. A. McLean, *Nanoscale*, 2012, **4**, 4269-4274.
37. H. Yang, J. Lei, B. Wu, Y. Wang, M. Zhou, A. Xia, L. Zheng and N. Zheng, *Chem. Commun.*, 2013, **49**, 300-302.
38. H. Yang, Y. Wang and N. Zheng, *Nanoscale*, 2013, **5**, 2674-2677.
39. A. Desireddy, B. E. Conn, J. Guo, B. Yoon, R. N. Barnett, B. M. Monahan, K. Kirschbaum, W. P. Griffith, R. L. Whetten, U. Landman and T. P. Bigioni, *Nature*, 2013, **501**, 399-402.
40. H. Yang, Y. Wang, H. Huang, L. Gell, L. Lehtovaara, S. Malola, H. Häkkinen and N. Zheng, *Nat Commun*, 2013, **4**.
41. I. Chakraborty, W. Kurashige, K. Kanehira, L. Gell, H. Häkkinen, Y. Negishi and T. Pradeep, *J. Phys. Chem. Lett.*, 2013, **4**, 3351-3355.
42. A. Desireddy, S. Kumar, J. Guo, M. D. Bolan, W. P. Griffith and T. P. Bigioni, *Nanoscale*, 2013, **5**, 2036-2044.
43. A. C. Dharmaratne, T. Krick and A. Dass, *J. Am. Chem. Soc.*, 2009, **131**, 13604-13605.
44. T. G. Schaaff and R. L. Whetten, *J. Phys. Chem. B*, 1999, **103**, 9394-9396.
45. U. Anand, S. Ghosh and S. Mukherjee, *J. Phys. Chem. Lett.*, 2012, **3**, 3605-3609.
46. A. Mathew and T. Pradeep, *Part. Part. Sys. Charac.*, 2014, DOI: 10.1002/ppsc.201400033.

-
47. S. K. Saikin, R. Olivares-Amaya, D. Rappoport, M. Stopa and A. Aspuru-Guzik, *Phys. Chem. Chem. Phys.*, 2009, **11**, 9401-9411.
48. B. Li, R.-W. Huang, J.-H. Qin, S.-Q. Zang, G.-G. Gao, H.-W. Hou and T. C. W. Mak, *Chem.–Eur. J.*, 2014, **20**, 12416-12420.
49. G. Li, Z. Lei and Q.-M. Wang, *J. Am. Chem. Soc.*, 2010, **132**, 17678-17679.
50. D. Sun, H. Wang, H.-F. Lu, S.-Y. Feng, Z.-W. Zhang, G.-X. Sun and D.-F. Sun, *Dalt. Trans.*, 2013, **42**, 6281-6284.
51. I. Casals, P. González-Duarte, J. Sola, J. Vives, M. Font-Bardia and X. Solans, *Polyhedron*, 1990, **9**, 769-771.
52. A. N. Parikh, S. D. Gillmor, J. D. Beers, K. M. Beardmore, R. W. Cutts and B. I. Swanson, *J. Phys. Chem. B*, 1999, **103**, 2850-2861.
53. C. C. McLauchlan and J. A. Ibers, *Inorg. Chem.*, 2001, **40**, 1809-1815.